Post-print of: Ryl J., Zieliński A., Bogdanowicz R., Darowicki K.: Heterogeneous distribution of surface electrochemical activity in polycrystalline highly boron-doped diamond electrodes under deep anodic polarization. ELECTROCHEMISTRY COMMUNICATIONS. Vol. 83, (2017), p. 41-45. DOI: 10.1016/j.elecom.2017.08.019

Heterogeneous distribution of surface electrochemical activity in polycrystalline highly boron-doped diamond electrodes under deep anodic polarization

Jacek Ryl[a] , Artur Zielinski[a], Robert Bogdanowicz[b], Kazimierz Darowicki[a]

[a] Department of Electrochemistry, Corrosion and Materials Engineering, Faculty of Chemistry, Gdansk University of Technology, 11/12 Narutowicza St., 80-233 Gdansk, Poland
[b] Department of Metrology and Optoelectronics, Faculty of Electronics, Telecommunications and Informatics, Gdansk University of Technology, 11/12 G. Narutowicza St., 80-233 Gdansk, Poland

ABSTRACT

The surface homogeneity of boron-doped diamond electrodes is variable and depends on anodic polarization conditions. The differentiation factor is the gradual and localized change in surface termination. A series of measurements under different polarization conditions was performed in order to investigate the scale of this effect. Nanoscale impedance microscopy (NIM) revealed large variation of surface resistance in individual grains. Based on the obtained results, we claim that the level of electrochemical heterogeneity significantly depends on the crystallographic texture of BDD. Modification of boron-doped diamond surface termination under anodic oxidation is assumed to be a multistage process.

Keywords: Boron-doped diamond, Surface oxidation, Electrochemical heterogeneity, Nanoscale impedance microscopy

1. Introduction

The majority of boron-doped diamond (BDD) electrodes in use are polycrystalline material, characterized by various grain sizes and boron dopant concentrations, which are directly influencing both local and global electric properties of these electrodes. The heterogeneity in electron-transfer rates of hydrogen terminated BDD (HT-BDD) is assumed to be mostly affected by non-uniform distribution of dopant throughout the film, preferential sp^2-carbon contamination in the inter-grain regions structural defects as well as the grain and interstitial boundaries size [1–7].

Behavior of BDD electrodes becomes more complex under electrochemical treatment, because of the presence of sp^2-carbon micro-domains, which undergo dynamic removal during cyclic polarization, thereby altering the overpotential of the oxygen evolution process [8,9]. Moreover, electrochemical treatment is a common procedure to acquire oxygen terminated (OT-BDD) electrodes [10–14]. HT-BDD possess much lower surface resistivity than OT-BDD due to the presence of a superficial conductive layer in hydrogenated diamond [10,12,15,16]. Anodic polarization influences the position of conduction and valence bands as a positive flat-band potential (E_{fb}) shift [17–21], hindering the charge transfer process by OT-BDD electrode, as revealed by impedance studies [10–12,22]. Still, several reports claim that extended polarization causes the dissociation of B–H pairs, and increases conductivity [13,14]. The formation of various oxygenated functional groups on the electrode surface can alter the electrochemically active sites and electron transfer for different adsorbed compounds. For example, when utilized for electrocatalytic processes, HT-BDD typically allows more homogeneous distribution of deposited particles [14,23–25]. Available sources report that PtNP/OT-BDD electrodes are more resistant to fouling during anodic treatment [24], while others reveal lower mechanical stability of AuNP/OT-BDD [26]. The complex nature of NPs/BDD interaction and the role of electrode termination require further studies.

The uncertainty of the overall heterogeneity level of individual electrodes often leads to the irreversibility of electrochemical processes or the lack of data reproducibility between different groups, in particular when surface-sensitive redox couples are used, such as $[Fe(CN)_6]^{4-/3-}$ [1,8,12,27,28]. Due to its non-uniform nature [1,29] BDD can be classified as an electrochemically heterogeneous electrode [30,31]. The current response of such systems depends on the shape and the time of development of the diffusion field in the vicinity sites with different activity [32,33]. The patterned microelectrode experiments confirmed the existence of discrepancies between the obtained results on the actual active surface and the estimated geometric one [33].

Crystallographic orientation of individual grains differentiates the electrode homogeneity, affecting the uptake of boron from the plasma

http://dx.doi.org/10.1016/j.elecom.2017.08.019

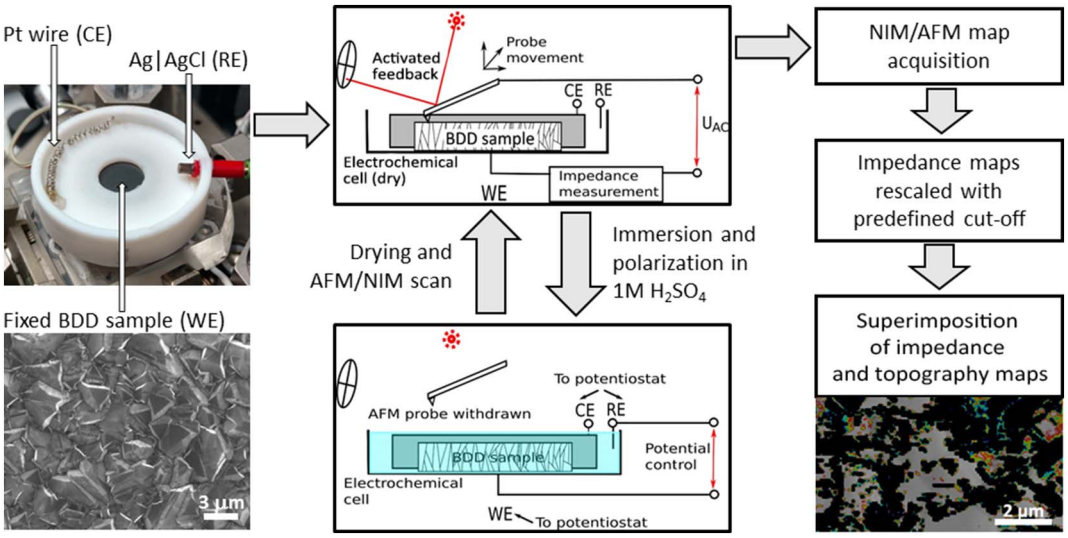

Fig. 1. Schematic representation of the applied experimental procedure and image processing.

phase in the specific facet (100, 110 or 111). The boron atoms incorporate at various substitutional sites, mainly contributing to the (111) growth sectors [7,34,35]. On the other hand, the lowest acceptor concentration occurs on the (100)-oriented faces [36,37]. This behavior was claimed as a possible reason behind a multistage mechanism of the observed oxidation process under anodic polarization [7,23,38]. Generally, the reactivity of particular surface region or facet of electrode is determined by several factors like the specific work function, number of Fermi level electrons or surface functionality etc. Due to significant variations between individual grains, one should take into consideration not only local heterogeneities at the grain boundary areas, but also the variable ratio of grain surfaces, in particular if the electrochemical treatment is applied [1]. The present work aims at evaluating development in electrode heterogeneity in relation to different conditions of anodic oxidation. It should be noted that applied measurements provide only electrical characterization of the BDD surface. Still, the results may contribute to the deeper understanding of the charge transfer process kinetics. Until now, the polarization-dependent BDD heterogeneity has not been reported.

2. Experimental

The boron-doped diamond electrodes (attn. 10,000 ppm [B]/[C] in plasma) were synthesized in an MWPECVD system (SEKI Technotron AX5400S, Japan) on p-type Si wafers as reported elsewhere [39,40]. A 6 h growth period produced microcrystalline diamond of ca. 2 µm in thickness, dominated by (110) and (111) facets, containing also (100) oriented crystals revealed by morphologic investigation [41–44]. XRD and EBSD analysis show highly randomized orientation of investigated BDD layers with no dominant texture and pole figures showing weak correlation with the (110) facets (not shown here). The applied pretreatment consisted of exposure to hot aqua regia and subsequently to microwave hydrogen plasma (1000 W, 300 sccm) to obtain H-terminated surface and to etch sp^2-carbon phase impurities, as reported elsewhere [17,45].

We have utilized novel multifrequency nanoscale impedance microscopy (NIM), which is a variation of AC signal probing implemented in contact mode atomic force microscopy (AFM) [46,47]. An impedance spectrum is attributed to each pixel of topographic image, enabling the determination of resistance maps (a sum of tip/sample contact and material spreading resistance). A similar approach was described in detail elsewhere [4]. Investigated samples underwent a topographic scan with a force of 1.24 µN, using commercially available BDD-coated conductive probes CDTP-NCHR (Nanosensors, Switzerland) [3,48]. The impedance and topography images were synchronously recorded. AFM tip shape quality was monitored by convolution measurements on TGT1 test sample [49]. Preliminary measurements show negligible impact of scanning procedure on HT-BDD surface resistance.

Prior to measurement, BDD samples were firmly mounted inside the electrochemical cell to ensure reproducibility of the analyzed area. The electrodes were immersed in 1 M H_2SO_4 and polarized under potentiostatic conditions for 20 min between the NIM scans. When the electrochemical treatment was applied, Ag|AgCl (+ 0.23 V vs SHE) served as a reference electrode, and platinum wire as a counter electrode. The polarization potential was equal to + 1.3; + 1.6; + 1.9; + 2.2 and + 2.5 V vs Ag|AgCl. Upon completion of anodic polarization, the electrolyte was poured out and the BDD electrodes were washed with deionized water, and then left to dry. The NIM scans were carried out consecutively to investigate changes in the electric properties of electrode surface. This procedure was repeated until each of the listed polarization potentials was imposed in ascending order.

Potentiostatic polarization was performed in the electrochemical cell (volume 2.5 cm^3) connected to NTegra Prima AFM system bipotentiostat (NT-MDT, Russia). The impedance analysis was performed in real time during the image acquisition process. The generation and acquisition of signal were performed by means of PXIe-4464 and PXIe-6124 cards (National Instruments, USA). Current sensing was performed with the use of SR 570 amplifier/filter (Stanford Research System, USA).

Once the NIM-derived maps were drawn, a threshold of 19.5 MΩ was applied to raise the contrast of resistance diversity between particular grains rather than (much larger variation) between the grain interiors and grain boundaries [1,4]. Finally, the topographic and resistance maps were superimposed for visualization purposes. The complete experimental procedure is schematically shown in Fig. 1.

High-resolution X-Ray Photoelectron Spectroscopy (XPS) measurements in C1s energy range were used to evaluate surface modification of Si/BDD electrodes using Escalab 250Xi (ThermoFisher Scientific, UK), equipped with Al-Kα source (spot diameter 650 µm). The energy step size and pass energy were 0.1 and 10 eV, respectively.

3. Results and discussion

AFM contour image (deflection) in Fig. 2a reveals the grain sizes and their distribution, while Fig. 2b–e presents the local resistance values obtained for one of the investigated BDD electrodes after consecutive anodic polarizations. The black areas on the NIM maps represent regions possessing resistance below the 19.5 MΩ threshold, and

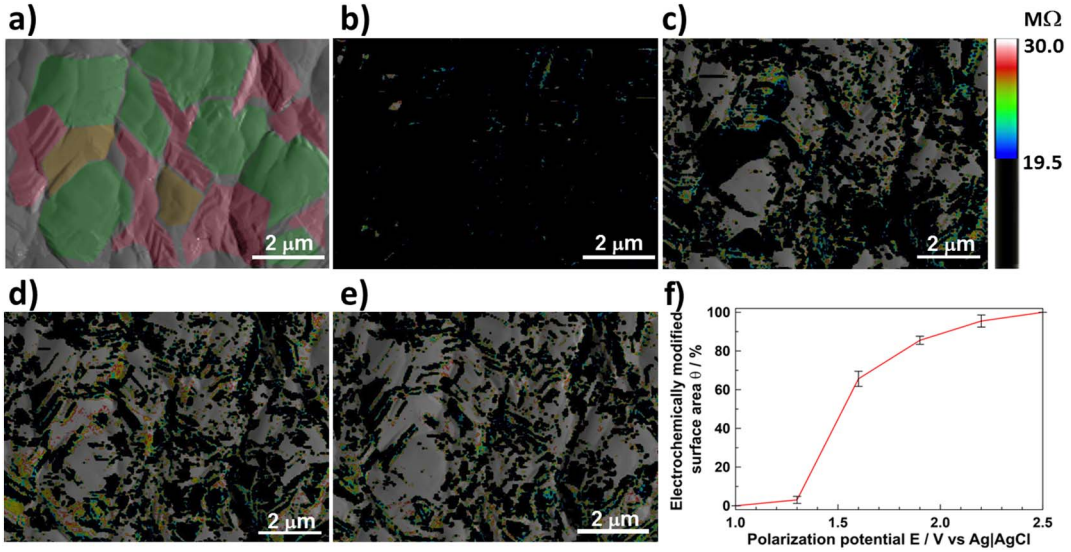

Fig. 2. a) AFM contour micrograph with superimposed colors to visualize the areas with varying tendency for surface oxidation, b–e) NIM map after a 20 min polarization at a given potential: b) 1.3 V, c) 1.6 V, d) 1.9 V, e) 2.5 V vs Ag|AgCl, f) electrochemically-modified surface area, θ. (For interpretation of the references to color in this figure legend, the reader is referred to the web version of this article.)

thus much higher surface conductivity than the transparent regions. Sample mounting enabled the observation of local changes in the exact same area each time.

Fig. 2b shows the surface resistance distribution after polarization at 1.3 V. The potential was too low to change the functionalization of BDD, therefore, it did not significantly alter the surface resistance. Deeper anodic polarization at 1.6 (Fig. 2c), 1.9 (Fig. 2d) and 2.5 V (Fig. 2e) resulted in a gradual increase in surface resistance. This increase was not homogeneous (neither was it linear), while its distribution corresponded to the shape of individual crystallites. In Fig. 2a, the areas possessing locally different electrochemical activity were marked with green, yellow and red colors. The areas marked in green revealed the surface modification at potentials as low as 1.6 V. The oxidation of orange and red areas required the application of higher potentials.

Electrochemically-modified surface area can be calculated as a fraction of surface area whose resistance falls below the applied threshold. This approach, based on the assumption that the lowest resistance dominates the charge transfer processes at the interface, was previously utilized in a similar study on the evaluation of electrochemically-active surface area, χ [3]. However, the changes of AFM tip conductivity during a series of consecutive scans and the resistance dispersion of different probes made it practically impossible to obtain the same conditions for repetitive measurements with different sensing elements. Therefore, a normalization procedure was needed to compare the individual BDD electrodes. Electrochemically-modified surface area can thus be calculated from Eq. (1):

$$\theta_{(E)} = \frac{1-\chi_{(E)}}{1-\chi_{2.5V}} * 100\% \quad (1)$$

where $(1-\chi_{(E)})$ is the electrochemically-transformed surface whose value depends on the probe conditions and applied threshold that vary between different measurements. Subsequently, $(1-\chi_{2.5V})$ is the fraction of surface transformed throughout the full measurement cycle for each individual electrode (typically in the 0.3–0.5 range). The observed variation of electrochemically-modified surface area at the nanoscale, θ, is presented in Fig. 2f. The experiment was repeated five times. The calculated error bars represent the variation of normalized electrochemically-modified surface area. One should note that θ refers only to a relative change of the surface area, used for normalization purposes.

An increase in area of higher resistance due to applied polarization is undoubtedly connected with oxidation of termination bonds, as the applied polarization range is sufficient for "mild" electrode oxidation [11,19,38]. It corroborates the fact that OT-BDD possess altered charge transfer kinetics and higher surface resistance [7,18,23,50,51] and should be concluded that certain grains are more prone to electrochemical modification than others.

Surface modification under polarization at < 1.6 V is negligible, while "mild" polarization at 1.6 V already leads to ca. 65% functionalization of the analyzed surface. Li et al. [52] reported that generally the [110] texture predominates in thick BDD films, while boron concentration in the film exhibits spatial inhomogeneity. Here, BDD is not characterized by major texture, while it is highly likely that dominant (110)-oriented planes are more prone toward oxidation at lower polarization potentials. Deeper anodic polarization successfully led to the oxidation of further crystallites. The electrochemical studies presented elsewhere [3] suggest a possibility that (111)-oriented planes might oxidize last, above 2.0 V. This would explain the shape of fractional oxidation rate function on Fig. 2f, also in good agreement with studies by Hoffmann et al. [23].

There is a strong indirect relationship between the surface oxidation tendency and flat-band potential, considering its values and ascending (110) > (100) > (111) order for different facets [37]. The above relationship underlies multistage surface modification hypothesis [3,38]. E_{fb} value depends on crystallographic orientation, boron dopant concentration and HT/OT termination type [17,19–21,36,42]. Zhao et al. [53] reported that B dopant increased the reactivity of adjacent H and OH and decreased the reactivity of adjacent O adsorbates. Therefore, it is surprising that (111)-orientated planes owing the highest boron dopant concentration are not the ones to oxidize at the lowest potentials.

High resolution XPS spectra recorded in the energy range of C1s made it possible to determine changes in surface chemistry under anodic polarization (Fig. 3). As a result of electrochemical surface modification, C1s shifts toward higher binding energies, reaching values similar to those of undoped diamond electrodes. This feature, described by Ballutaud et al. [15] in relation to the removal of conductive superficial layer during oxidation processes, corroborates well the NIM results. The most often used fitting procedure consists of three to four different components. The first component (C_1) is centered around a value of 284.1 eV, and can be attributed to the hydrogenated layer present on the surface of the as-prepared electrode. The second component (C_2) is usually shifted by + 0.8 eV, and is associated with

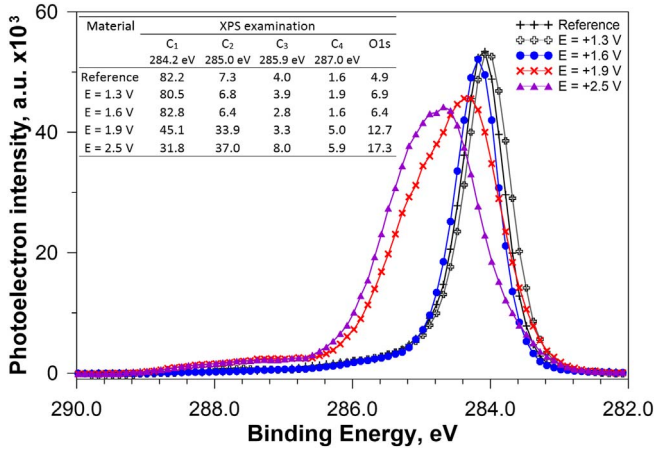

Fig. 3. High-resolution XPS spectra in the energy range of C1s measured for each investigated sample. Table in the inset presents chemical analysis after deconvolution.

non-hydrogenated carbon atoms. Finally, as a result of surface oxidation, the (C_3) and (C_4) components emerge which are shifted by + 1.7 and + 2.8 eV, respectively [38,54–56]. The latter two correspond to the C—OH (hydroxyl) bonds, but also ether, carbonyl and/or carboxyl bonds. The observed modification of surface chemistry is in agreement with NIM data.

4. Conclusions

We have found that local surface electric properties greatly depend on the conditions of anodic polarization process, which can contribute explanation of the well-known lack of reproducibility in polarization studies and prove the existence of the multistage mechanism of oxidation process. The NIM/AFM studies revealed heterogeneity of surface conductivity between the individual electrochemically-modified diamond grains. The degree of changes is dependent on the polarization level.

A decrease in conductivity should be associated with the formation of OT-terminations. The (110)-oriented facets tend to be more easily oxidized. They have the largest share in the surface area, resulting in the strongest impact on the overall electrode behavior. Much deeper anodic polarization is required to oxidize differently oriented grains. The results obtained suggest the following oxidation order: (110) > (100) > (111), while it should be noted that the hypothesis is based upon presumptive evidence.

On the basis of our findings, surface oxidation tendency as well as boron dopant concentration appears to be interdependent on the crystallographic orientation of individual grains, while not directly affecting each other. As a result, local oxidation of functional groups gradually changes the overall electrochemical and physico-chemical properties of BDD material. This is a key factor influencing the surface functionalization with target-specific molecules or charge transfer, e.g. in bio-sensors or energy harvesting and electroanalytical devices and thus further studies of this phenomenon are essential.

Acknowledgments

This work was supported by the National Science Centre of Poland [grant numbers: 2015/17/D/ST5/02571, 2014/14/M/ST5/00715, 2016/21/B/ST7/01430, 2016/21/B/ST7/01439] and DS funds of Faculty of Electronics, Telecommunications and Informatics, Gdansk University of Technology.

References

[1] K.B. Holt, A.J. Bard, Y. Show, G.M. Swain, Scanning electrochemical microscopy and conductive probe atomic force microscopy studies of hydrogen-terminated boron-doped diamond electrodes with different doping levels, J. Phys. Chem. B 108 (2004) 15117–15127, http://dx.doi.org/10.1021/jp048222x.

[2] T. Kolber, K. Piplits, R. Haubner, H. Hutter, Quantitative investigation of boron incorporation in polycrystalline CVD diamond films by SIMS, Fresenius J. Anal. Chem. 365 (1999) 636–641, http://dx.doi.org/10.1007/s002160051537.

[3] J. Ryl, A. Zielinski, L. Burczyk, R. Bogdanowicz, T. Ossowski, K. Darowicki, Chemical-assisted mechanical lapping of thin boron-doped diamond films: a fast route toward high electrochemical performance for sensing devices, Electrochim. Acta 242 (2017) 268–279, http://dx.doi.org/10.1016/j.electacta.2017.05.027.

[4] A. Zielinski, R. Bogdanowicz, J. Ryl, L. Burczyk, K. Darowicki, Local impedance imaging of boron-doped polycrystalline diamond thin films, Appl. Phys. Lett. 105 (2014) 131908, http://dx.doi.org/10.1063/1.4897346.

[5] D. Becker, K. Juttner, Influence of surface inhomogeneities of boron doped CVD-diamond electrodes on reversible charge transfer reactions, J. Appl. Electrochem. 33 (2003) 959–967, http://dx.doi.org/10.1023/A:1025872013482.

[6] D. Becker, K. Juttner, The impedance of fast charge transfer reaction on boron doped diamond electrodes, Electrochim. Acta 49 (2003) 29–39, http://dx.doi.org/10.1016/j.electacta.2003.04.003.

[7] N.R. Wilson, S.L. Clewes, M.E. Newton, P.R. Unwin, J.V. Macpherson, Impact of grain-dependent boron uptake on the electrochemical and electrical properties of polycrystalline boron doped diamond electrodes, J. Phys. Chem. B 110 (2006) 5639–5646, http://dx.doi.org/10.1021/jp0547616.

[8] L.A. Hutton, J.G. Iacobini, E. Bitziou, R.B. Channon, M.E. Newton, J.V. Macpherson, Examination of the factors affecting the electrochemical performance of oxygen-terminated polycrystalline boron-doped diamond electrodes, Anal. Chem. 85 (2013) 7230–7240, http://dx.doi.org/10.1021/ac401042t.

[9] M.H.P. Santana, L.A. De Faria, J.F.C. Boodts, Electrochemical characterisation and oxygen evolution at a heavily boron doped diamond electrode, Electrochim. Acta 50 (2005) 2017–2027, http://dx.doi.org/10.1016/j.electacta.2004.08.050.

[10] M. Wang, N. Simon, C. Decorse-Pascnut, M. Bouttemy, A. Etcheberry, M. Li, R. Boukherroub, S. Szunerits, Comparison of the chemical composition of boron-doped diamond surfaces upon different oxidation processes, Electrochim. Acta 54 (2009) 5818–5824, http://dx.doi.org/10.1016/j.electacta.2009.05.037.

[11] J. Ryl, R. Bogdanowicz, P. Slepski, M. Sobaszek, K. Darowicki, Dynamic electrochemical impedance spectroscopy (DEIS) as a tool for analyzing surface oxidation processes on boron-doped diamond electrodes, J. Electrochem. Soc. 161 (2014) H359–H364, http://dx.doi.org/10.1149/2.016406jes.

[12] S. Carlos Oliveira, A.M. Oliveira-Bret, Voltammetric and electrochemical impedance spectroscopy characterization of a cathodic and anodic pre-treated boron doped diamond electrode, Electrochim. Acta 55 (2010) 4599–4605, http://dx.doi.org/10.1016/j.electacta.2010.03.016.

[13] P.C. Ricci, A. Anedda, C.M. Carbonaro, F. Clemente, R. Corpino, Electrochemically induced surface modifications in boron-doped diamond films: a Raman spectroscopy study, Thin Solid Films 482 (2005) 311–317, http://dx.doi.org/10.1016/j.tsf.2004.11.169.

[14] T. Spataru, L. Preda, C. Munteanu, A.I. Caciuleanu, N. Spataru, A. Fujishima, Influence of boron-doped diamond surface termination on the characteristics of titanium dioxide anodically deposited in the presence of a surfactant, J. Electrochem. Soc. 162 (2015) H535–H540, http://dx.doi.org/10.1149/2.0741508jes.

[15] D. Ballutaud, N. Simon, H. Girard, E. Rzepka, B. Bouchet-Fabre, Photoelectron spectroscopy of hydrogen at the polycrystalline diamond surface, Diam. Relat. Mater. 15 (2006) 716–719, http://dx.doi.org/10.1016/j.diamond.2006.01.004.

[16] H. Girard, E. de La Rochefoucauld, D. Ballataud, A. Etcheberry, N. Simon, Controlled anodic treatments on boron-doped diamond electrodes monitored by contact angle measurements, Electrochem. Solid-State Lett. 10 (2007) F34–F37, http://dx.doi.org/10.1149/1.2743824.

[17] H.B. Suffredini, V.A. Pedrosa, L. Codognoto, S.A.S. Machado, R.C. Rocha-Filho, L.A. Avaca, Enhanced electrochemical response of boron-doped diamond electrodes brought on by a cathodic surface pre-treatment, Electrochim. Acta 49 (2004) 4021–4026, http://dx.doi.org/10.1016/j.electacta.2004.01.082.

[18] P. Actis, A. Denoyelle, R. Boukherroub, S. Szunerits, Influence of the surface termination on the electrochemical properties of boron-doped diamond (BDD) interfaces, Electrochem. Commun. 10 (2008) 402–406, http://dx.doi.org/10.1016/j.elecom.2007.12.032.

[19] H. Girard, N. Simon, D. Ballutaud, M. Herlem, A. Etcheberry, Effect of Anodic and Cathodic Treatments on the charge transfer of boron doped diamond electrodes, Diam. Relat. Mater. 16 (2007) 316–325, http://dx.doi.org/10.1016/j.diamond.2006.06.009.

[20] H. Girard, N. Simon, D. Ballutaud, E. de La Rochefoucauld, A. Etcheberry, Effects of controlled anodic treatments on electrochemical behaviour of boron doped diamond, Diam. Relat. Mater. 16 (2007) 888–891, http://dx.doi.org/10.1016/j.diamond.2006.12.002.

[21] T.N. Rao, D.A. Tryk, K. Hashimoto, A. Fujishima, Band-edge movements of semiconducting diamond in aqueous electrolyte induced by anodic surface treatment, J. Electrochem. Soc. 146 (1999) 680–684, http://dx.doi.org/10.1149/1.1391662.

[22] E. Vanhove, J. de Sanoit, J.C. Arnault, S. Saada, C. Mer, P. Mailley, P. Bergonzo, M. Nesladek, Stability of H-terminated BDD electrodes: an insight into the influence of the surface preparation, Phys. Status Solidi A 204 (2007) 2931–2939, http://dx.doi.org/10.1002/pssa.200776340.

[23] R. Hoffmann, H. Obloh, N. Tokuda, N. Yang, C.E. Nebel, Fractional surface termination of diamond by electrochemical oxidation, Langmuir 28 (2012) 47–50, http://dx.doi.org/10.1021/la2039366.

[24] T. Spataru, P. Osiceanu, M. Anastasescu, G. Patrinolu, C. Munteanu, N. Spataru, A. Fujishima, Effect of the chemical termination of conductive diamond substrate

on the resistance to carbon monoxide-poisoning during methanol oxidation of platinum particles, J. Power Sources 261 (2014) 86–92, http://dx.doi.org/10.1016/j.jpowsour.2014.03.044.
[25] D.A. Tryk, K. Tsunozaki, T.N. Rao, A. Fujishima, Relationships between surface character and electrochemical processes on diamond electrodes: dual roles of surface termination and near-surface hydrogen, Diam. Relat. Mater. 10 (2001) 1804–1809, http://dx.doi.org/10.1016/S0925-9635(01)00453-8.
[26] J. Svanberg-Larsson, G.W. Nelson, S. Escobar Steinvall, B.F. Leo, E. Brooke, D.J. Payne, J.S. Foord, A comparison of explicitly-terminated diamond electrodes decorated with gold nanoparticles, Electroanalysis 28 (2016) 88–95, http://dx.doi.org/10.1002/elan.201500442.
[27] I. Duo, A. Fujishima, Ch. Comninellis, Electron transfer kinetics on composite diamond (sp^3)-graphite (sp^2) electrodes, Electrochem. Commun. 5 (2003) 695–700, http://dx.doi.org/10.1016/S1388-2481(03)00169-3.
[28] G.P. Morris, A.N. Simonov, E.A. Mashkina, R. Bordas, K. Gillow, R.E. Baker, D.J. Gavaghan, A.M. Bond, A comparison of fully automated methods of data analysis and computer assisted heuristic methods in an electrode kinetic study of the pathologically bariable $[Fe(CN)_6]^{3-/4-}$ process by AC voltammetry, Anal. Chem. 85 (2013) 11780–11787, http://dx.doi.org/10.1021/ac4022105.
[29] G.R. Salazar-Banda, K.I.B. Eguiluz, A.E. de Carvalho, L.A. Avaca, Ultramicroelectrode array behavior of electrochemically partially blocked boron-doped diamond surface, J. Braz. Chem. Soc. 24 (7) (2013) 1206–1211, http://dx.doi.org/10.5935/0103-5053.20130141.
[30] T.J. Davies, R.R. Moore, C.E. Banks, R.G. Compton, The cyclic voltammetric response of electrochemically heterogeneous surfaces, J. Electroanal. Chem. 574 (2004) 123–152, http://dx.doi.org/10.1016/j.jelechem.2004.07.031.
[31] T.J. Davies, C.E. Banks, R.G. Compton, Voltammetry at spatially heterogeneous electrodes, J. Solid State Electrochem. 9 (2005) 797–808, http://dx.doi.org/10.1007/s10008-005-0699-x.
[32] K. Jüttner, D. Becker, Characterization of boron-doped diamond electrodes by electrochemical impedance spectroscopy, J. Appl. Electrochem. 37 (2006) 27–32, http://dx.doi.org/10.1007/s10800-006-9228-6.
[33] B.A. Brookes, T.J. Davies, A.C. Fisher, R.G. Evans, S.J. Wilkins, K. Yunus, J.D. Wadhawan, R.G. Compton, Computational and experimental study of the cyclic voltammetry response of partially blocked electrodes. Part 1. Nonoverlapping, uniformly distributed blocking systems, J. Phys. Chem. B 107 (2003) 1616–1627, http://dx.doi.org/10.1021/jp021810v.
[34] R. Samlenski, C. Haug, R. Brenn, C. Wild, R. Locher, P. Koidl, Characterization and lattice location of nitrogen and boron in homoepitaxial CVD diamond, Diam. Relat. Mater. 5 (1996) 947–951, http://dx.doi.org/10.1016/0925-9635(95)00471-8.
[35] J.C. Richley, J.N. Harvey, M.N.R. Ashfold, Boron incorporation at a diamond surface: a QM/MM study of insertion and migration pathways during chemical vapor deposition, J. Phys. Chem. C 116 (2012) 18300–18307, http://dx.doi.org/10.1021/jp305773d.
[36] Y.V. Pleskov, Y.E. Evstefeeva, M.D. Krotova, V.P. Varnin, I.G. Teremetskaya, Synthetic semiconductor diamond electrodes: Electrochemical behaviour of homoepitaxial boron-doped films orientated as (111), (110), and (100) faces, J. Electroanal. Chem. 595 (2006) 168–174, http://dx.doi.org/10.1016/j.jelechem.2006.07.010.
[37] Y.V. Pleskov, Y.E. Evstefeeva, V.P. Varnin, I.G. Teremetskaya, Synthetic semiconductor diamond electrodes: electrochemical characteristics of homoepitaxial boron-doped films grown at the (111), (110), and (100) faces of diamond crystals, Russ. J. Electrochem. 40 (2004) 886–892, http://dx.doi.org/10.1023/B:RUEL.0000041354.70107.c8.
[38] J. Ryl, L. Burczyk, R. Bogdanowicz, M. Sobaszek, K. Darowicki, Study on surface termination of boron-doped diamond electrodes under anodic polarization in H_2SO_4 by means of dynamic impedance technique, Carbon 96 (2016) 1093–1105, http://dx.doi.org/10.1016/j.carbon.2015.10.064.
[39] M. Sobaszek, L. Skowronski, R. Bogdanowicz, K. Siuzdak, A. Cirocka, P. Zieba, M. Gnyba, M. Naparty, L. Golunski, P. Plotka, Optical and electrical properties of ultrathin transparent nanocrystalline boron-doped diamond electrodes, Opt. Mater. 42 (2015) 24–34, http://dx.doi.org/10.1016/j.optmat.2014.12.014.
[40] R. Bogdanowicz, M. Sawczak, P. Niedzialkowski, P. Zieba, B. Finke, J. Ryl, J. Karczewski, T. Ossowski, Novel functionalization of boron-doped diamond by microwave pulsed-plasma polymerized allylamine film, J. Phys. Chem. C 118 (2014) 8014–8025, http://dx.doi.org/10.1021/jp5003947.
[41] K. Siuzdak, R. Bogdanowicz, M. Sawczak, M. Sobaszek, Enhanced capacitance of composite TiO_2 nanotube/boron-doped diamond electrodes studied by impedance spectroscopy, Nanoscale 7 (2015) 551–558, http://dx.doi.org/10.1039/c4nr04417g.
[42] R. Bogdanowicz, Characterization of optical and electrical properties of transparent conductive boron-doped diamond thin films grown on fused silica, Metrol. Meas. Syst. 21 (2014) 685–698, http://dx.doi.org/10.2478/mms-2014-0059.
[43] Z.L. Wang, C. Lu, J.J. Li, C.Z. Gu, Effect of gas composition on the growth and electrical properties of boron-doped diamond films, Diam. Relat. Mater. 18 (2009) 132–135, http://dx.doi.org/10.1016/j.diamond.2008.10.040.
[44] C.H. Goetling, F. Marken, A. Gutierrez-Sosa, R.G. Compton, J.S. Foord, Electrochemically induced surface modifications of boron-doped diamond electrodes: an X-ray photoelectron spectroscopy study, Diam. Relat. Mater. 9 (2000) 390–396, http://dx.doi.org/10.1016/S0925-9635(99)00267-8.
[45] L. Codognoto, S.A.S. Machado, L.A. Avaca, Square wave voltammetry on boron-doped diamond electrodes for analytical determinations, Diam. Relat. Mater. 11 (2002) 1670–1675, http://dx.doi.org/10.1016/S0925-9635(02)00134-6.
[46] L.S.C. Pingree, E.F. Martin, K.R. Shull, M.C. Hersam, Nanoscale impedance microscopy - a characterization tool for nanoelectronic devices and circuits, IEEE Trans. Nanotechnol. 4 (2005) 255, http://dx.doi.org/10.1109/TNANO.2004.837856.
[47] K. Darowicki, A. Zieliński, K.J. Kurzydłowski, Application of dynamic impedance spectroscopy to atomic force microscopy, Sci. Technol. Adv. Mater. 9 (2008) 045006 http://dx.doi.org/10.1088/1468-6996/9/4/045006.
[48] A. Zieliński, K. Darowicki, Implementation and validation of multisinusoidal, fast impedance measurements in atomic force microscope contact mode, Microsc. Microanal. 20 (2014) 974–981, http://dx.doi.org/10.1017/S1431927614000531.
[49] A. Yacoot, L. Koenders, Aspects of scanning force microscope probes and their effects on dimensional measurement, J. Phys. D. Appl. Phys. 41 (2008) 103001 http://dx.doi.org/10.1088/0022-3727/41/10/103001.
[50] D. Medeiros de Araujo, P. Canizares, C.A. Martinez-Huitle, M.A. Rodrigo, Electrochemical conversion/combustion of a model organic pollutant on BDD anode: role of sp^3/sp^2 ratio, Electrochem. Commun. 47 (2014) 37–40, http://dx.doi.org/10.1016/j.elecom.2014.07.017.
[51] M. Yang, J.S. Foord, X. Jiang, Diamond electrochemistry at the nanoscale: a review, Carbon 99 (2016) 90–110, http://dx.doi.org/10.1016/j.carbon.2016.11.061.
[52] H. Li, T. Zhang, L. Li, X. Lu, B. Li, Z. Jin, G. Zou, Investigation on crystalline structure, boron distribution, and residual stresses in freestanding boron-doped CVD diamond films, J. Cryst. Growth 312 (2010) 1986–1991, http://dx.doi.org/10.1016/j.jcrysgro.2010.03.020.
[53] S. Zhao, K. Larsson, Theoretical study of the energetic stability and geometry of terminated and B-doped diamond (111) surfaces, J. Phys. Chem. C 118 (2014) 1944–1957, http://dx.doi.org/10.1021/jp409278x.
[54] H. Girard, N. Simon, D. Ballutaud, A. Etcheberry, Correlation between flat-band potential position and oxygenated termination nature on boron-doped diamond electrodes, C. R. Chim. 11 (2008) 1010–1015, http://dx.doi.org/10.1016/j.crci.2008.01.014.
[55] M. Wang, E. Simon, G. Charrier, M. Bouttemy, A. Etcheberry, M. Li, R. Boukherroub, S. Szunerits, Distinction between surface hydroxyl and ether groups on boron-doped diamond electrodes using a chemical approach, Electrochem. Commun. 12 (2010) 351–354, http://dx.doi.org/10.1016/j.elecom.2009.12.029.
[56] P. Niedzialkowski, R. Bogdanowicz, P. Zieba, J. Wysocka, J. Ryl, M. Sobaszek, T. Ossowski, Melamine-modified boron-doped diamond towards enhanced detection of adenine, guanine and caffeine, Electroanalysis 28 (2015) 211–221, http://dx.doi.org/10.1002/elan.201500528.